COUPLING OF ELECTRODIALYSIS AND BIO-ELECTROCHEMICAL SYSTEMS FOR METAL AND ENERGY RECOVERY FROM ACID MINE DRAINAGE

Y. Delgado, J. Llanos, F. J. Fernández-Morales*

Department of Chemical Engineering. Faculty of Chemical Sciences and Technologies. University of Castilla La Mancha. Campus Universitario s/n. 13071 Ciudad Real. Spain.

* Corresponding author: Francisco Jesús Fernández Morales

University of Castilla-La Mancha, ITQUIMA, Chemical Engineering Dept., Avda. Camilo José Cela S/N 13071, Ciudad Real, Spain.

Tel: 0034 926 295300 (ext. 6350), Fax: 0034 926 295242.

E-mail: fcojesus.fmorales@uclm.es

Orcid iD: 0000-0003-0389-6247

Abstract

BACKGROUND: This work study the treatment of a synthetic sphalerite acid mine drainage (AMD). The treatment was carried out by means of a previous concentration stage, by using electrodialysis, and a subsequent electrodeposition by using bioelectrochemical system (BES).

RESULTS: Operating the electrodialysis at 8V and at a diluate/concentrate volume ratio of 3 the best concentration results were obtained. This treatment yielded a concentrate fraction of about 25% of the volume and a clear fraction of about 75% of the volume. The concentrated fraction was treated in a BES to electrodeposite the metal contained. Operating as microbial fuel cell (MFC), the spontaneous reactions took place and in 2 days all the Fe^{3+} was reduced to Fe^{2+}, then all the Cu^{2+} was electrodeposited as pure Cu^{0} in about 8 d. The maximum current density attained in this stage was 0.1 mA cm^{-2} and the maximum power was 0.05 W cm^{-2}. Then, a subsequent operation as microbial electrolysis cell (MEC) allowed to simultaneously recover the Fe^{2+}, Ni^{2+}, Zn^{2+}, Mn^{2+} and Cd^{2+} as a mixed metal mass.

CONCLUSION: The electrodialysis yielded a clear effluent representing 75% of the total volume and a concentrated effluent accounting for 25%. It was possible to treat the concentrated effluent in a MFC recovering pure Cu^{0} with a net electricity generation. The non-spontaneous metal reductions were subsequently accomplished by means of MEC, being the electricity requirements lower than in the case of the raw AMD because of the higher mass transfer rate and the reduction of the Ohmic loses.

Keywords

Acid mine drainage; Electrodialysis; Microbial fuel cell; Microbial electrolysis cell; Metal recovery; Energy generation

1. INTRODUCTION

According to the report of the European Environment Agency for promoting the transition to a sustainable Europe, it could exist 2.8 million polluted places in the European Union, although only 24% of them listed. In this report, it is stated that past mining activities are one of the main responsible for the pollution of water bodies due to the leaching of metals from abandoned polluted soils (1). In this scenario, the management of abandoned mines represent an environmental issue of increasing concern due to the pollution of both soils and water bodies.

Regarding Spain, there are 73 installations which contain dangerous mine residues, according to the last actualization of the Spanish Ministry for Ecological Transition (2). Among the different effluents and polluted soils that are produced from abandoned mining facilities, acid mine drainage (AMD) is probably those that represents the highest potential hazard to the environment (3). As its name indicates, the AMD has an acidic pH (between 1 and 4) that is produced by the contact between the polluted soil and rainwater, producing puddles contaminated with metal ions (4).

AMD treatment technologies can be classified into passive or active technologies. The formers are focused on reducing the environmental impact by neutralization with alkaline effluents (5,6), the use of microorganisms (7), permeable reactive barriers (8), the application of artificial wetlands (9,10) or phytoremediation (11,12). Nevertheless, this option has the disadvantage of the greater time required to achieve the desired objectives. Though, the sludge generated is more stable, and its operational costs and maintenance are more affordable (13).

Active technologies imply higher operational and maintenance costs, but their performance generally overcomes passive technologies. In this group are included ion exchange processes (14), membrane technologies (15–17) or adsorption processes (18).

74 Within the group of processes that can be applied for the recovery of metals from mine
75 effluents, electrochemical and bioelectrochemical processes, including Microbial Fuel Cell
76 (MFC) and Microbial Electrolysis Cells (MEC) stand out as promising alternatives (19).
77 Thus, several studies have researched the performance of MFC on the recovery of AMD,
78 with the simultaneous recovery of iron deposits a goethite (20). Also working with a MFC
79 system, Zhang et al. recently studied the mechanism of copper removal, evaluating the
80 effect of current, pH and copper concentration on the recovery of copper from polluted
81 wastewater (21). With a system working as MEC, Luo et al. demonstrated the viability of
82 recovering Cu^{2+}, Ni^{2+} and Fe^{2+} from AMD solutions, being able to simultaneously produce
83 hydrogen (22). An interesting approach was performed by Sun and coworkers, who
84 proposed the fabrication of iron oxide catalyst for electro-Fenton reaction from the
85 recovery of iron from AMD (23). More recently, Rodrigues et al. propose the use of
86 electrocoagulation for the recovery of sulphate and the control of pH from AMD, reporting
87 an efficiency of 70.95% in the process (24).
88 An additional electrochemical technology that has been previously used for the recovery of
89 AMD is electrodialysis. With this electro-membrane process, it is possible to remove up to
90 97% of the metals present in an AMD (25). In the same line, Martí-Calatayud and
91 coworkers proposed the recovery of sulfuric acid from AMD in the anion compartment of
92 an electrodialysis cell (26). One of the limitations found in both works was the increase in
93 the cell voltage due to the precipitation of iron hydroxide on the surface of the cation-
94 exchange membranes. An additional limitation is the fact that any membrane process (as it
95 is the case of electrodialysis) represents a proper alternative for water recovery but cannot
96 provide a selective metal recovery, as it was stated by Naidu et al. in their recent review
97 about the remediation, reuse and resource recovery from AMD effluents (8).
98 In previous works of our research group, the treatment of AMD was confronted by a
99 bioelectrochemical system that was sequentially operated as a microbial fuel cell (MFC)

and, subsequently, as a microbial electrolysis cell (MEC) (27,28). In these systems, the cathode of the bioelectrochemical system was fed with AMD solution meanwhile the anode was fed with a solution of sodium acetate and was inoculated with a mixed culture population taken from the biological reactor of the conventional wastewater treatment plant of Ciudad Real (Spain). More information about this facility can be found elsewhere (29). According to the results obtained in these works, Fe^{3+} is selectively reduced to Fe^{2+} and Cu^{2+} reduced to metallic copper within the stage of MFC, obtaining a maximum power density of 0.0134 mW cm^{-2}. The rest of metals (Fe, Ni and Sn) can be recovered within the subsequent MEC operation, with reduced electric consumption due to the contribution of the electroactive bacteria located at the anode.

Based on the findings and on the lacks detected in previous studies focused on the field, in the present work we proposed the recovery of metals from AMD by a combination of an electromembrane process (electrodialysis) and a subsequent bioelectrochemical operation as MFC and MEC. The main variables affecting the electrodialysis process, applied voltage and concentrate/dilate ratio, were studied. The concentrate solution obtained from the electrodialysis stage was fed to the bioelectrochemical system and the metal recovery and energy implications were studied. The combined electrodialysis-MFC/MEC technology would provide treated water from the electrodialysis process, electricity production and metal recovery from the MFC as well as enhanced metal recovery from the MEC due to the higher metal concentration of the AMD.

2. MATERIALS AND METHODS

2.1. Electrodialysis

The experimental electrodialysis set-up used in this work is a commercial PCCell® (PCCell GmbH, Heusweiler, Germany) assembled with 4 cell-pairs and fully described elsewhere (30). Each membrane has a surface area of 69 cm^2, being both anode and

126 cathode square meshes (56.25 cm^2 of geometric area) made of mixed mineral oxides
127 (MMO, IrO_2-RuO_2). This cell was operated in a 3 compartments scheme: diluate,
128 concentrate and electrode rinsing solution (anolyte and catholyte were mixed). Both diluate
129 and concentrate compartments were fed with the target synthetic AMD used in this work
130 (concentration shown in Table 1), meanwhile 2 g L^{-1} sodium sulphate solution was used
131 for electrode rinsing.

132 Table 1. Synthetic AMD composition.

Ion	**Ion Concentration (mg L^{-1})**	**Salt**
Cu^{2+}	100	$CuSO_4 \cdot 5H_2O$
Fe^{3+}	100	$Fe_2(SO_4)_3 \cdot H_2O$
Ni^{2+}	30	$NiSO_4 \cdot 6H_2O$
Zn^{2+}	3,000	$ZnSO_4 \cdot 7H_2O$
Mn^2	200	$MnSO_4 \cdot H_2O$
Cd^{2+}	80	$CdSO_4 \cdot 8/3H_2O$

133

134 Each experiment lasted 240 minutes at constant voltage (from 2 to 8 V). The volume of
135 diluate compartment was fixed 1.5 L, meanwhile concentrate volume was varied from 0.5
136 to 1.5 L, in order to study the influence of the diluate/concentrate volume ratio on the
137 performance of the system. The concentration of all metals listed in Table was measured
138 by Inductively Coupled Plasma Mass Spectrometer ICP-MS, Thermo electron X-series II.
139 Moreover, the evolution of conductivity (EC-Meter Crison GLP 31), pH (pH meterCrison
140 GLP 22) and current intensity (Digital Multimeter 60.131 Electro DH) was monitored
141 throughout the tests.

142

2.2 Bio-Electrochemical Cells

The experimental set-up used in this stage consisted in two Bio-Electrochemical Systems (BES) cells and an abiotic blank cell treating the concentrated AMD obtained after the electrodialysis. The abiotic blank test was used to isolate the chemical processes by avoiding the activity of the microbial culture. All the BES systems used were composed by two chambers, anodic and cathodic, of 100 mL each one. These compartments were separated by a bipolar membrane (Fumasep® FBM) and connected by an external electrical circuit loaded with a resistor of 120 Ω. The BES reactors were made of transparent PVC, the compartments were sealed by using silicon gaskets in order to prevent liquid leakages. The anode was made of carbon felt (KFA10, SGL Carbon Group), 2.5 x 2.5 x 1.1 cm. This material was selected because, according to the literature, presents better performance than other carbon based electrodic materials for the biofilm creation (27,28). The cathode was made of titanium, 2.5 x 2.5 cm. Titanium was used as cathodic material because of its corrosion resistance on acidic environments, such that presented by the AMD, and because metals can be recovered easily from their surface without damaging the electrode [30]. The BES were operated at room temperature.

Before the treatment of the concentrated AMD, it was necessary to create a biofilm on the carbon felt used as anodic electrode. To do that, the anolyte was filled 50% with activated sludge from a domestic wastewater treatment plant located in Ciudad Real, more information can be found elsewhere (31), and 50% with a medium, which is composed by 1 $g \cdot L^{-1}$ CH_3COONa, 3 $g \cdot L^{-1}$ Na_2HPO_4, 0.7 $g \cdot L^{-1}$ KH_2PO_4, 0.8 $g \cdot L^{-1}$ $(NH_4)_2SO_4$, 0.2 $g \cdot L^{-1}$ $MgCl_2 \cdot 6H_2O$, 0.05 $g \cdot L^{-1}$ $CaCl_2$ and 0.04 $g \cdot L^{-1}$ $(NH_4)_2Fe(SO_4)_2 \cdot 6H_2O$. In the literature it has been described that the biofilm growth and energy production are favored by acetate, because of that it is easily consumed as carbon source in BES systems (32). The fresh anodic medium had a pH of 7 and a conductivity of 4.27 $mS \cdot cm^{-1}$. Before the tests, with the aim to facilitate the biofilm development, the catholyte was filled with a supporting

electrolyte, 4 $g \cdot L^{-1}$ Na_2SO_4 and aerated in order to ensure oxygen saturation and therefore to enhance the oxygen reduction reaction. Working in this way, the high performance of the cathode facilitates the biofilm development at the anode. The biofilm development took about one month. Once the biofilm was developed, the supporting electrolyte of the catholyte was replaced by the concentrated AMD obtained after the electrodialysis treatment. The anolyte was cyclically replaced when consumed by fresh medium, these cycles took about 3 days. Therefore, the abiotic BES test was started when the biotic cells were fed with the concentrated AMD. Every time the fresh medium was fed, the anode was purged with nitrogen gas to ensure anaerobic conditions before the anodic reactions took place. For the abiotic cell, the acclimation stage was not required because no biofilm was required. Anyway, to mimic the chemical conditions, the abiotic anode was purged with nitrogen gas to ensure anaerobic condition.

For the treatment of concentrated AMD with BESs systems, the electrochemical cells were first operated as MFCs for 288 hours to take advantage of the spontaneous bio-electro chemical processes. Then, the BES was operated as MECs for 240 hours. The MEC operation was divided in three stages that operated at different cathodic potentials: -0.5 V for 48 hours, -1 V for 96 h and finally at -1.5 V for 96 hours.

Every day, 1 mL of catholyte sample was taken and analyzed to measure the total concentration of the metals studied Cu, Zn, Cd Ni and Fe by using an Inductively Coupled Plasma Mass Spectrometer ICP-MS, Thermo electron X-series II. The Cu^{2+} and Fe^{2+} concentrations were determined by Sprectroquant Pharo 100 Merck spectrophotometer through copper and iron test method, respectively. Fe^{3+} concentration was obtained by the difference between total iron obtained by ICP and Fe^{2+} by spectrophotometry. The cell voltage and intensity for MFC and MEC were automatically recorded every minute for each cell by Keithley 2000 multimeter connected to KickStart software for on-line data storage.

195 The cathodic electrodes were characterized, before and after the experiments, by using
196 High Resolution Scanning Electron Microscopy (HRSEM) coupled with Energy
197 Dispersive X-Ray Spectroscopy (EDS) detector using a ZEISS GeminiSEM 500
198 Microscope. X-Ray diffraction measurements were realized by a Philips X'Pert MPD with
199 Kα radiation from copper radiation, λ = 1.54056 Å, with graphite monochromator and
200 xenon gas sealed detector. Operations conditions were 2 theta angle between 3 and 100º
201 with a sweep speed of $0.05^{\circ} \cdot s^{-1}$. Then, Philips X'Pert HighScore Plus software was used to
202 compare the diffraction patterns with the Joint Committee on Powder Diffraction
203 Standards database.
204
205 **3. RESULTS AND DISCUSSION**
206 **3.1. Treatment of AMD by electrodialysis**
207 The influence of applied voltage on the time course of the concentration of zinc, nickel,
208 iron, copper and cadmium concentrations is presented in Figure 1. Due to the dissimilar
209 values of initial concentration of the different metals, all values have been referred to the
210 initial concentration of each ion.

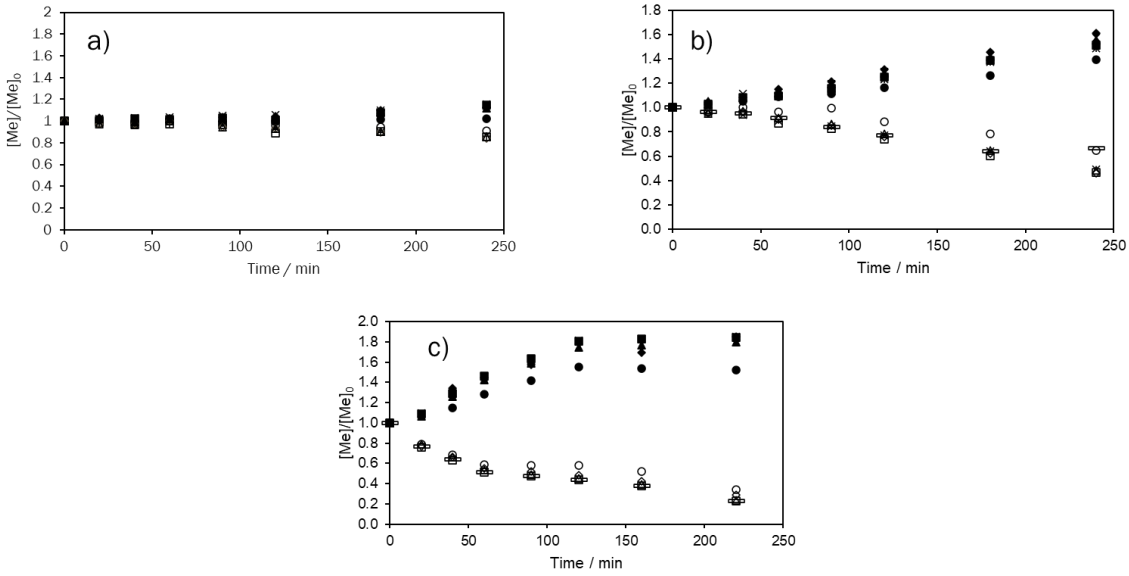

Figure 1. Influence of applied voltage on time course of Zn, Ni, Fe, Cu and Cd relative concentration in both concentrate (C) and diluate (D) compartments. Concentrate volume (1.5 L); Diluate volume (1.5 L).

a) 2 V, b) 4 V and c) 8 V

x Zn,C; - Zn,D; ■ Ni,C; □ Ni,D; ● Fe,C; ○ Fe,D; ♦ Cu,C; ◊ Cu,D; ▲ Cd,C; Δ Cd,D; * Mn, C; + Mn,D.

As it can be observed, a higher rate in the transport of metal ions is obtained when higher potentials are applied. This result is basically explained by an increasing driving force that promotes the movement of ions through the ion-exchange membranes and is typical of electrodialysis processes that are not working under mass transfer limitations (33,34). At an applied potential of 8 V (2 V per cell pair) it is possible to reduce the concentration of all ions of the initial effluent until 20 % of its initial value at 240 min of operation time without observing noticeable mass transfer limitations or membrane fouling. It is worth noting that this value of voltage is considerably lower than similar previous works, where applied voltages up to 13 V per cell pair were applied (35).

An additional conclusion that can be obtained from Figure 1 is that the system presents scarce selectivity on the separation of the metals present in the initial effluent. The only ion that exhibits a slightly lower mobility towards the ion exchange membranes is iron, as its concentration in the diluate compartment throughout the test performed at 8V is slightly higher than the rest of metal ions. Specifically, the final concentration of iron in this test is 0.344 (ratio with respect to its initial concentration) meanwhile the rest of metal ions reached an average final concentration ratio of 0.247. The mobility of metal ions through ion exchange membranes mainly depends on the size, charge and speciation of the metals under consideration (35). In this work, all metals presented similar sizes because their atomic number ranging from 25 and 48. The ions sizes in order from smallest to largest were the following: Cd<Zn<Cu<Ni<Fe<Mn. Additionally, at the operational conditions in this work, the iron use to be present as Fe^{3+} oxyhydroxide (36,37), which significantly increases it size, reducing therefore its transport across the membrane in the electrodialysis tests (38).

Previous works that presented higher selectivity toward the mobility of different ions (which is not the aim of the present work) applied a modified electrodialysis system by using complexing agents as EDTA (39) or by the manufacturing of special membranes with enhanced selectivity (33).

Considering these results, a potential of 8 V was selected as the most appropriate to perform the following stage on the optimization of the electrodialysis process, which consists of increasing the diluate/concentrate (D/C) volume ratio in order to reach a higher degree of concentration of the solution to be used as the feed stream of the bioelectrochemical process. Thus, Figure 2 shows the influence of this volume ratio on the time course of all metal ions.

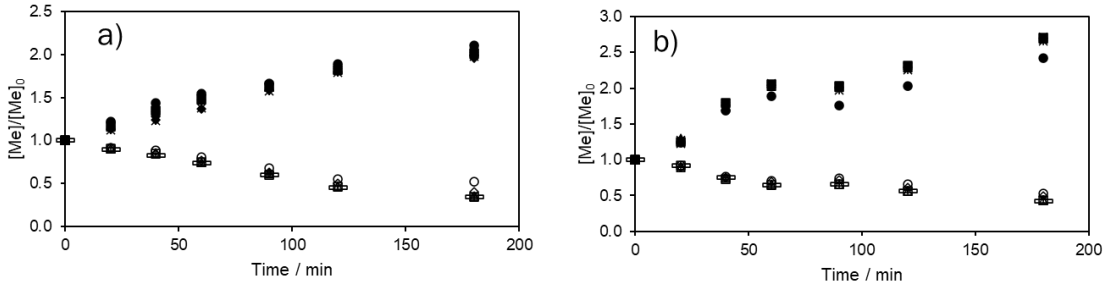

Figure 2. Influence of volume ratio diluate/concentrate on time course of Zn, Ni, Fe, Cu and Cd relative concentration in both concentrate (C) and diluate (D) compartments. a) Diluate volume: 1.5 L; Concentrate volume: 1.0 L b) Diluate volume: 1.5 L; Concentrate volume: 0.5 L.

x Zn,C; - Zn,D; ■ Ni,C; □ Ni,D; ● Fe,C; ○ Fe,D; ♦ Cu,C; ◊ Cu,D; ▲ Cd,C; Δ Cd,D; *Mn, C; + Mn,D. Applied voltage: 8 V.

As it can be observed, it is possible to increase the volumetric diluate/concentrate ratio to 3 maintaining the capacity of the system to generate a concentrated solution and without observing a noticeable decrease on the rate of the concentration process. Working with this ratio, it would be possible to produce 75% of a treated effluent from the incoming AMD and 25% of a concentrated solution, with a concentration approximately three-fold that of the influent.

In order to select the optimal conditions for the operation of the electrodialysis cell, the electric consumption per order for electrodialysis (E_{ED}) was determined. This parameter is defined as the electric consumption needed to decrease the concentration of the diluate compartment by one order of magnitude calculated per unit volume of treated effluent (diluate). This parameter can be calculated by using Equation 1, adapted from (40) considering that intensity is not constant thorough the electrodialysis tests:

$$E_{ED} = \frac{E_{cell} \cdot \int_0^{t_f} I \cdot t \cdot dt}{V \cdot log\left({}^{c_0}/_{c_f}\right)}$$

Where, E_{cell} refers to the applied potential (V), I is the measured intensity (A), t_f is final time of the test (h), V is diluate volume (L) and C_0 and C_f are initial and final average concentration of the metal ions treated (M). Thus, Figure 3 shows the influence of the concentrate/diluate volume ratio in the E_{ED}.

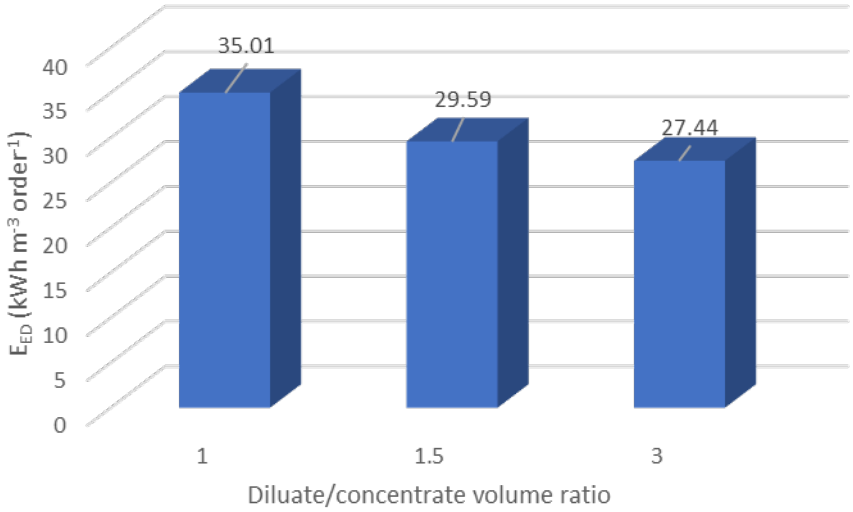

Figure 3. Influence of volume ratio diluate/concentrate on electric consumption per order for the concentration of metal ions of AMD by electrodialysis. Applied voltage: 8 V.

As it can be observed, there is a decrease on power consumption when increasing diluate to concentrate volume ratio. The decrease on the power consumption is related to the lower intensity registered throughout the test at the highest volume ratio, as the final degree of dilution reached, the applied voltage and the diluate volume were equal for all tests. The estimated specific power consumption per order is 27.44 kWh m^{-3} for the highest volume ratio tested (the largest possible taking into account system limitations). This behavior, together with the fact that the highest volume ratio implies the highest degree of concentration in the concentrate compartment and the lowest volume of the concentrated stream, makes this volume ratio optimal for performing the concentration of the AMD effluent by electrodialysis.

3.2. Bio-electrodeposition of concentrated AMD

As previously indicated, the concentrated AMD obtained working at the optimal conditions was subjected to metal recovery by using BES technology.

In Table SM1 the thermodynamic reduction potential values of the metals studied in this work as well as the corresponding to the fuel used in the anode, acetate, are presented. As can be seen in this table, the reduction potentials of Cu^{2+} to Cu^{0} and Fe^{3+} to Fe^{2+}, 0.040 and 0.549 V vs Ag/AgCl, respectively, are over the anode potential at OCP conditions, −0.524 V vs Ag/AgCl. Therefore, the reduction reaction of Cu^{2+} to Cu^{0} and Fe^{3+} to Fe^{2+}, should occur spontaneously. However, the reduction reactions of Fe^{2+}, Sn^{2+} and Ni^{2+} are under the anode potential at OCP conditions and, therefore, should not take place spontaneously. Because of the spontaneity of the bio-electrochemical reactions, the BES operation had two stages. The first stage, in which the spontaneous reactions took place, was carried out with operating the BES system as MFC. The second stage was carried out operating the BES system as MEC, with external energy supply, in order to achieve the non-spontaneous reduction reactions. During the MFC stage, spontaneous anodic and cathodic reactions took place generating a maximum voltage of 55 mV, a maximum current density of 0.1 mA cm^{-2} and a maximum power of 0.05 W cm^{-2}. These values were higher than those described in the literature when operated in similar conditions, a maximum current density of 0.136 mA cm^{-2} and a maximum power density of 0.0134 mW cm^{-2} (41). These results could be explained because the higher metal concentration facilitated the mass transference processes and reduced the Ohmic loses of the electrochemical process (42). The anodic spontaneous reaction was the oxidation of the acetate dosed to the anode by the mixed microbial culture, whereas the cathodic spontaneous reactions were the metal reduction reactions, Cu^{2+} to Cu^{0} and Fe^{3+} to Fe^{2+}.

315 In Figure 4, it can be seen the evolution of the current density exerted by the MFC during
316 the operation. The changes in the current density marked with an arrow corresponds to the
317 dosification of fresh anodic medium.

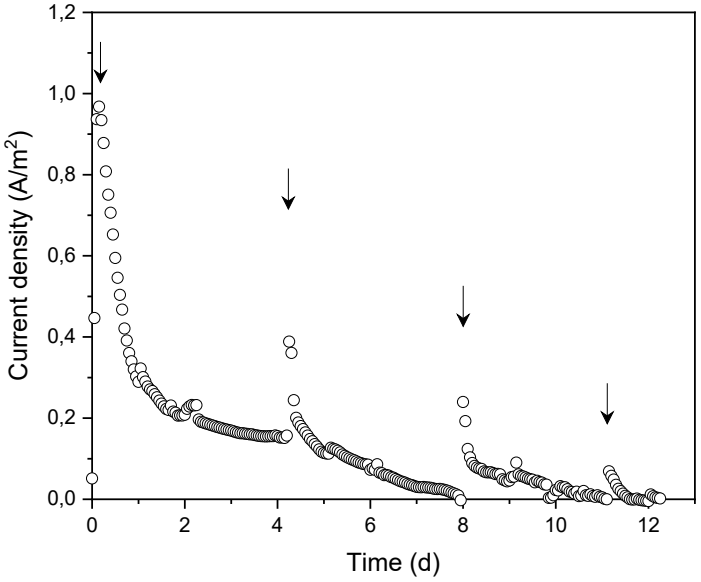

318

319 Figure 4. Current density generated during the MFC operation.

320

321 As can be seen in Figure 4, the current density exerted decreased along the experiment
322 despite feeding additional carbon substrate, acetate, to the anode. This behavior can be
323 explained because of the fully consumption of the metals able to be spontaneously reduced
324 at the cathode. Taking into account the electrical behaviour of the MFC, the Fe^{3+} reduction
325 to Fe^{2+} and the Cu^{2+} reduction to Cu^{0}, reactions which take place at 0.5487 and 0.0398 V
326 versus Ag/AgCl, respectively, were the sole spontaneous reduction reactions taking place
327 during the MFC operation. The rest of the metals contained in the concentrated AMD
328 presented lower reduction potentials and were not spontaneously reduced at the cathode. In
329 Figure 5, it is presented the evolution of the Fe^{3+} and the Cu^{2+} along the MFC operation.
330 As can be seen in Figure 5a, during the first two days, most of the Fe^{3+} was reduced to
331 Fe^{2+}. Once finished the Fe^{3+} to Fe^{2+} reduction, the Cu^{2+} to Cu^{0} reduction reaction started.

After about 8 d, see Figure 5b, all the Cu^{2+} contained in the concentrated AMD was reduced to Cu^0, removing the cooper from the AMD and recovering it on the surface of the cathodic electrode due to the bio-electrodeposition process. After 12 d, the Cu recovery was finished, and no cathodic spontaneous reactions took place in the cathode. This behavior was previously predicted by the exerted current density, which plummet to zero after 12 d of operation, in spite of the acetate dosification at the anode, indicating the absence of cathodic spontaneous reactions.

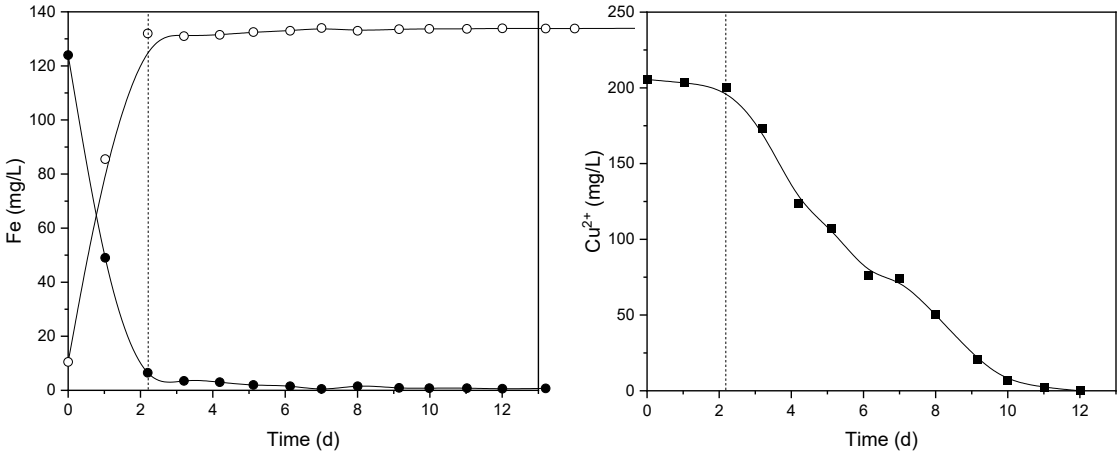

Figure 5. Metal concentration in the liquid bulk during the biotic MFC operation. ○ Fe^{2+}; ● Fe^{3+}; ▲ Fe precipitated; ■ Cu^{2+}.

In the case of the abiotic cell no reduction reaction took place and therefore no voltage was exerted, and no metal was neither reduced nor recovered. After the 12 d of operation, a slight brownish color was observed in the liquid bulk. Because of the lack of electrogenic activity at the abiotic cell, the color generation could be explained by the generation of metal colloids due to the high pH, 7.2, presented by the concentrated solution. The colloids mainly involved ferric iron, being the iron removal caused by the colloids formation negligible. In the literature, it has been previously described that when the pH of the AMD increased above 3.5, precipitates primarily composed of ferric iron are obtained. These

354 precipitates are yellow-to-red-to-brown in color and have long been referred to as “yellow
355 boy” by North American miners (43).
356 The acetate concentration at the anode was measured before the anolyte replacement. In all
357 the cases the acetate consumption was lower than 60% which ensured the acetate
358 availability at the anode during the MFC operation The Acetate removal at the abiotic
359 anode was negligible, this was the expected result because the anodic oxidation of acetate
360 is a non-spontaneous reaction in absence of the electrogenic microbial culture which
361 catalyze the reaction.
362 In order to characterize the cathode after the MFC operation, the biotic and abiotic
363 cathodes were characterized by means of XRD analysis and SEM, see Figure 6. As can be
364 seen in this Figure, the abiotic MFC does not recover any Cu, being the only signal
365 identified that of the titanium electrode. However, the biotic tests presented two additional
366 peaks due to the Cu recovery and the iron manganese oxide dragged by the Cu
367 electrodeposition. In the literature, similar structures have been described (44) when
368 recovering copper by means of MFC systems.
369

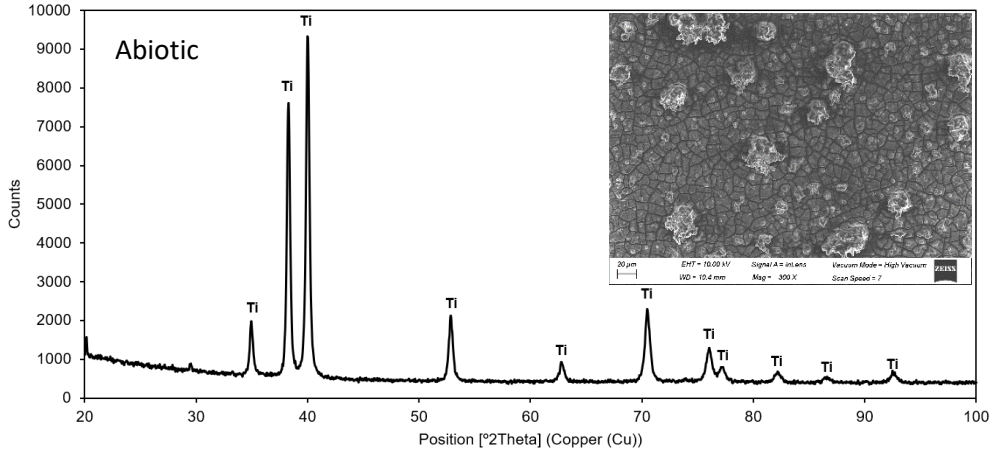

370

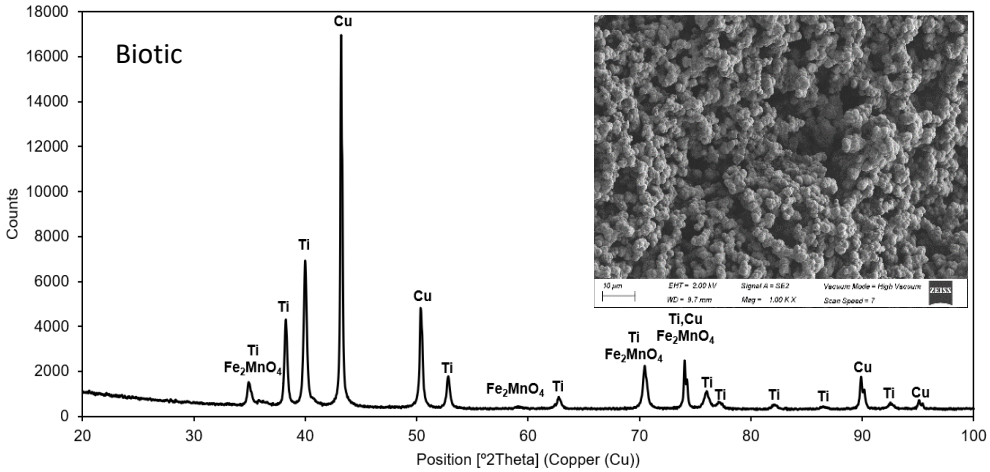

Figure 6. XRD analysis of cathode after the MFC operation. SEM images of the cathode of the abiotic and biotic MFC.

Once finished the spontaneous reactions, the BES systems were operated as MEC with the aim to recover the rest of metals contained in the AMD. During the MEC operation different voltages were imposed in order to study the dependence of the metal deposition with the cathode potential. The cathode potentials applied were -0.5, -1.0 and -1.5 V versus Ag/AgCl, conditions of limiting current for the electroreduction of the metals remaining in the AMD. In Figure 7, it is presented the current density obtained during the MEC operation. As can be seen in Figure 7, the current was maintained along the whole process indicating metal electrodeposition at the cathode.

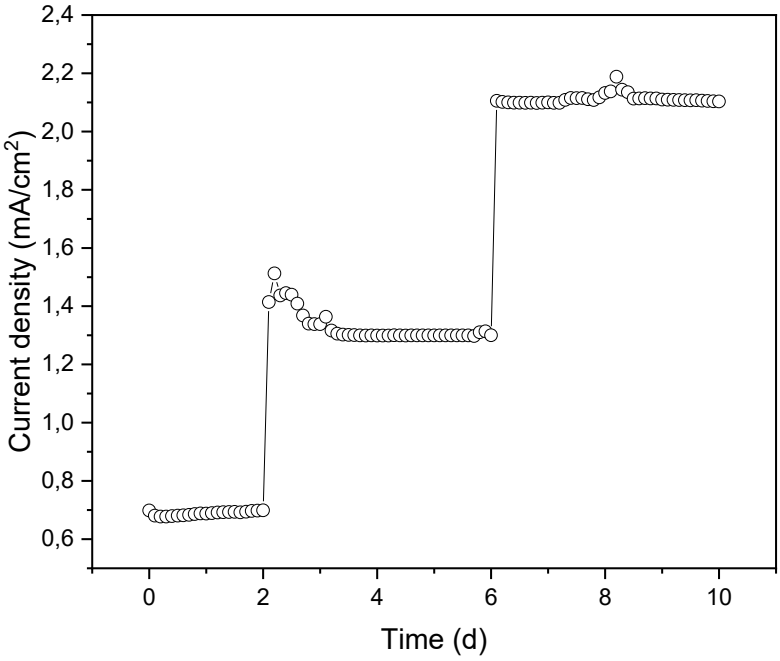

Figure 7. Current density during the MEC operation.

When operating at -0.5 V a negligible metal electrodeposition was observed despite the current density observed 0.7 mA/cm^2. When operating at -1.0 V a mixed metal electrodeposition of zinc, manganese, cadmium, nickel and iron was observed causing a current density of 1.3 mA/cm^2. Finally, at -1.5 V the manganese and traces of iron and zinc were electrodeposited causing a current density of 2.1 mA/cm^2. The increased current density exerted could be explained because of the increase of the electro-active area of the cathode due to the metal electrodeposition on the surface of the cathode (45) as well as the decrement of the activation overpotential after the metal electrodeposition onto the electrode surface (41). During all the stages of the MEC operation, a mixed metal electrodeposition was observed on the surface of the cathode, being not possible to carry out a selective metal recovery within the cathode potentials applied in this work.

4. CONCLUSIONS

The coupling of electrodialysis and BES systems allows to energy and material valorization of the metal polluted in the synthetic sphalerite AMD used in this work. The optimum operational conditions for the electrodialysis were a dilute/concentrate volume ratio of 3 and an applied voltage of 8 V. The concentrated effluent obtained accounted for 25 of the initial volume. This concentrated solution was fed to BES system in order to extract the chemical energy and recover the metals. All the Cu^{2+} contained in the concentrated AMD was recovered as Cu^0 after 10 d of operation. The maximum current density attained in this stage was 0.1 mA cm^{-2} and the maximum power exerted was 0.05 W cm^{-2}, values higher than those obtained when operating with diluted AMD.

Then the non-spontaneous reactions were accomplished by operating as MEC, after 10 d all the metals were recovered as mixed metals, being impossible a selective recover with the potentials applied. The energy required was lower than that required for the electrodeposition of the diluted AMD due to the reduction of the ohmic loses and the increase of the mass transfer processes.

In that way, the previous concentration of the AMD increased the quality of the effluent obtained in both the electrodialysis and the BES operation, increasing at the same time the energy valorisation when operating as MFC.

Acknowledgements

Financial support from the following sources is gratefully acknowledged: Project SBPLY/19/180501/000254 from European Union (FEDER) and Castilla-La Mancha regional government, and Projects PID2019-107282RB-I00 and EQC2018-004240-P from Ministry of Science, Innovation and Universities.

Bibliography

1. European Environment Agency. The European environment-state and outlook 2020 Knowledge for transition to a sustainable Europe [Internet]. Available from: http://europa.eu

2. Ministerio para la Transición Ecológica y el Reto Demográfico - Minería [Internet]. [cited 2021 Nov 12]. Available from: https://energia.gob.es/mineria/Mineria/Paginas/Mineria.aspx

3. Viadero RC, Zhang S, Hu X, Wei X. Mine drainage: Remediation technology and resource recovery. Vol. 92, Water Environment Research. John Wiley and Sons Inc; 2020. p. 1533–40.

4. Rodríguez L, Ruiz E, Alonso-Azcárate J, Rincón J. Heavy metal distribution and chemical speciation in tailings and soils around a Pb-Zn mine in Spain. J Environ Manage. 2009 Feb;90(2):1106–16.

5. Tolonen ET, Sarpola A, Hu T, Rämö J, Lassi U. Acid mine drainage treatment using by-products from quicklime manufacturing as neutralization chemicals. Chemosphere. 2014;117(1):419–24.

6. Goel RK, Flora JR v., Chen JP. Flow Equalization and Neutralization. In: Physicochemical Treatment Processes. 2005.

7. Peiravi M, Mote SR, Mohanty MK, Liu J. Bioelectrochemical treatment of acid mine drainage (AMD) from an abandoned coal mine under aerobic condition. J Hazard Mater. 2017;333:329–38.

8. Naidu G, Ryu S, Thiruvenkatachari R, Choi Y, Jeong S, Vigneswaran S. A critical review on remediation, reuse, and resource recovery from acid mine drainage. Vol. 247, Environmental Pollution. Elsevier Ltd; 2019. p. 1110–24.

9. Pat-Espadas AM, Portales RL, Amabilis-Sosa LE, Gómez G, Vidal G. Review of constructed wetlands for acid mine drainage treatment. Vol. 10, Water (Switzerland). MDPI AG; 2018.

10. Guzman M, Romero Arribasplata MB, Flores Obispo MI, Bravo Thais SC. Removal of heavy metals using a wetland batch system with carrizo (phragmites australis (cav.) trin. ex steud.): A laboratory assessment. Acta Ecologica Sinica. 2021 Aug;

11. Muthusaravanan S, Sivarajasekar N, Vivek JS, Paramasivan T, Naushad M, Prakashmaran J, et al. Phytoremediation of heavy metals: mechanisms, methods and enhancements. Vol. 16, Environmental Chemistry Letters. Springer Verlag; 2018. p. 1339–59.

12. Nagy A, Magyar T, Juhász C, Tamás J. Phytoremediation of acid mine drainage using by-product of lysine fermentation. Water Science and Technology. 2020 Apr 1;81(7):1507–17.

13. Simate GS, Ndlovu S. Acid mine drainage: Challenges and opportunities. Vol. 2, Journal of Environmental Chemical Engineering. Elsevier Ltd; 2014. p. 1785–803.

14. Felipe ECB, Batista KA, Ladeira ACQ. Recovery of rare earth elements from acid mine drainage by ion exchange. Environmental Technology (United Kingdom). 2021;42(17):2721–32.

15. Al-Zoubi H, Rieger A, Steinberger P, Pelz W, Haseneder R, Härtel G. Optimization study for treatment of acid mine drainage using membrane technology. Sep Sci Technol. 2010;45(14):2004–16.

16. Ambiado K, Bustos C, Schwarz A, Bórquez R. Membrane technology applied to acid mine drainage from copper mining. Water Science and Technology. 2017 Feb 1;75(3):705–15.

17. Agboola O. The role of membrane technology in acid mine water treatment: a review. Vol. 36, Korean Journal of Chemical Engineering. Springer New York LLC; 2019. p. 1389–400.

18. Dlamini CL, de Kock LA, Kefeni KK, Mamba BB, Msagati TAM. Polymeric ion exchanger supported ferric oxide nanoparticles as adsorbents for toxic metal ions from aqueous solutions and acid mine drainage. J Environ Health Sci Eng. 2019 Jul 1;17(2):719–30.

19. Rodríguez-Galán M, Baena-Moreno FM, Vázquez S, Arroyo-Torralvo F, Vilches LF, Zhang Z. Remediation of acid mine drainage. Vol. 17, Environmental Chemistry Letters. Springer Verlag; 2019. p. 1529–38.

20. Cheng S, Jang JH, Dempsey BA, Logan BE. Efficient recovery of nano-sized iron oxide particles from synthetic acid-mine drainage (AMD) water using fuel cell technologies. Water Res. 2011;45(1):303–7.

21. Zhang J, Huang S, Gao XT, Wang H, Cao X, Li X. Influence mechanism of heavy metal removal under microcurrent action. Sep Purif Technol. 2021 May 15;263.

22. Luo H, Liu G, Zhang R, Bai Y, Fu S, Hou Y. Heavy metal recovery combined with H2 production from artificial acid mine drainage using the microbial electrolysis cell. J Hazard Mater. 2014 Apr 15;270:153–9.

23. Sun M, Ru XR, Zhai LF. In-situ fabrication of supported iron oxides from synthetic acid mine drainage: High catalytic activities and good stabilities towards electro-Fenton reaction. Appl Catal B. 2015 Apr 1;165:103–10.

24. Rodrigues C, Follmann HVDM, Núñez-Gómez D, Nagel-Hassemer ME, Lapolli FR, Lobo-Recio MÁ. Sulfate removal from mine-impacted water by electrocoagulation: statistical study, factorial design, and kinetics. Environmental Science and Pollution Research. 2020 Nov 1;27(31):39572–83.

25. Buzzi DC, Viegas LS, Rodrigues MAS, Bernardes AM, Tenório JAS. Water recovery from acid mine drainage by electrodialysis. Vol. 40, Minerals Engineering. Elsevier Ltd; 2013. p. 82–9.

26. Martí-Calatayud MC, Buzzi DC, García-Gabaldón M, Ortega E, Bernardes AM, Tenório JAS, et al. Sulfuric acid recovery from acid mine drainage by means of electrodialysis. Desalination. 2014;343.

27. Leon-Fernandez LF, Medina-Díaz HL, Pérez OG, Romero LR, Villaseñor J, Fernández-Morales FJ. Acid mine drainage treatment and sequential metal recovery by means of bioelectrochemical technology. Journal of Chemical Technology and Biotechnology. 2021 Jun 1;96(6):1543–52.

28. León-Fernandez LF, Rodríguez Romero L, Fernández-Morales FJ, Villaseñor Camacho J. Modelling of a bioelectrochemical system for metal-polluted wastewater treatment and sequential metal recovery. Journal of Chemical Technology and Biotechnology. 2021 Jul 1;96(7):2033–41.

29. Rodríguez Mayor L, Villaseñor Camacho J, Fernández Morales FJ. Operational optimisation of pilot scale biological nutrient removal at the Ciudad Real (Spain) domestic wastewater treatment plant. Water Air Soil Pollut. 2004;152(1–4).

30. Llanos J, Cotillas S, Cañizares P, Rodrigo MA. Novel electrodialysis-electrochlorination integrated process for the reclamation of treated wastewaters. Sep Purif Technol. 2014 Aug 20;132:362–9.

31. Rodríguez Mayor L, Villaseñor Camacho J, Fernández Morales FJ. Operational optimisation of pilot scale biological nutrient removal at the Ciudad Real (Spain) domestic wastewater treatment plant. Water Air Soil Pollut. 2004;152(1–4):279–96.

32. Mateo S, Cañizares P, Rodrigo MA, Fernandez-Morales FJ. Driving force behind electrochemical performance of microbial fuel cells fed with different substrates. Chemosphere. 2018;207.

33. Saravanan A, Kumar PS, Hemavathy R v., Jeevanantham S, Harikumar P, Priyanka G, et al. A comprehensive review on sources, analysis and toxicity of environmental pollutants and its removal methods from water environment. Science of the Total Environment. 2022 Mar 15;812.

34. Raschitor A, Llanos J, Cañizares P, Rodrigo MA. Novel integrated electrodialysis/electro-oxidation process for the efficient degradation of 2,4-dichlorophenoxyacetic acid. Chemosphere. 2017;182:85–9.

35. Kim J, Yoon S, Choi M, Min KJ, Park KY, Chon K, et al. Metal ion recovery from electrodialysis-concentrated plating wastewater via pilot-scale sequential electrowinning/chemical precipitation. J Clean Prod. 2022 Jan 1;330.

36. España JS. The behavior of iron and aluminum in acid mine drainage. Speciation, mineralogy, and environmental significance. In: Thermodynamics, Solubility and Environmental Issues. 2007.

37. Garg S, Jiang C, Waite TD. Impact of pH on Iron Redox Transformations in Simulated Freshwaters Containing Natural Organic Matter. Environ Sci Technol. 2018;52(22).

38. Stenina I, Golubenko D, Nikonenko V, Yaroslavtsev A. Selectivity of transport processes in ion-exchange membranes: Relationship with the structure and methods for its improvement. Vol. 21, International Journal of Molecular Sciences. 2020.

39. Babilas D, Muszyński J, Milewski A, Leśniak-Ziółkowska K, Dydo P. Electrodialysis enhanced with disodium EDTA as an innovative method for separating Cu(II) ions from zinc salts in wastewater. Chemical Engineering Journal. 2021 Mar 15;408.

40. Lanzarini-Lopes M, Garcia-Segura S, Hristovski K, Westerhoff P. Electrical energy per order and current efficiency for electrochemical oxidation of p-chlorobenzoic acid with boron-doped diamond anode. Chemosphere. 2017;188:304–11.

41. Leon-Fernandez LF, Medina-Díaz HL, Pérez OG, Romero LR, Villaseñor J, Fernández-Morales FJ. Acid mine drainage treatment and sequential metal recovery by means of bioelectrochemical technology. Journal of Chemical Technology and Biotechnology. 2021;96(6).

42. Garche J. Encyclopedia of Electrochemical Power Sources. Encyclopedia of Electrochemical Power Sources. 2009.

43. Bigham JM, Nordstrom DK. Iron and aluminum hydroxysulfates from acid sulfate waters. In: Sulfate Minerals: Crystallography, Geochemistry, and Environmental Significance. 2019.

44. Heijne A ter, Liu F, Weijden R van der, Weijma J, Buisman CJN, Hamelers HVM. Copper recovery combined with electricity production in a microbial fuel cell. Environ Sci Technol. 2010 Jun 1;44(11):4376–81.

45. Pletcher D, Greff R, Peat R, Peter LM, Robinson J. Instrumental methods in electrochemistry. Instrumental methods in electrochemistry. 2001.